Electronic Supplementary Material (ESI) for Journal of Materials Chemistry A.

Ligand modification of Cu_2ZnSnS_4 nanoparticles boosts the performance of low temperature paintable carbon electrode based perovskite solar cells to 17.71%

Yang Cao[a], Weiwei Li[b], Zhen Liu[a], Zhiqiang Zhao[a], Zhenyu Xiao[a], Wei Zi[a], Nian Cheng[a]*,

[a] Energy-Saving Building Materials Collaborative Innovation Center of Henan Province, Xinyang Normal University, 237 Nanhu Road, Xinyang, 464000, China

[b] College of Physics and Electronic Engineering, Xinyang Normal University, 237 Nanhu Road, Xinyang, 464000, China

*Corresponding author

Email: chengnian@foxmail.com

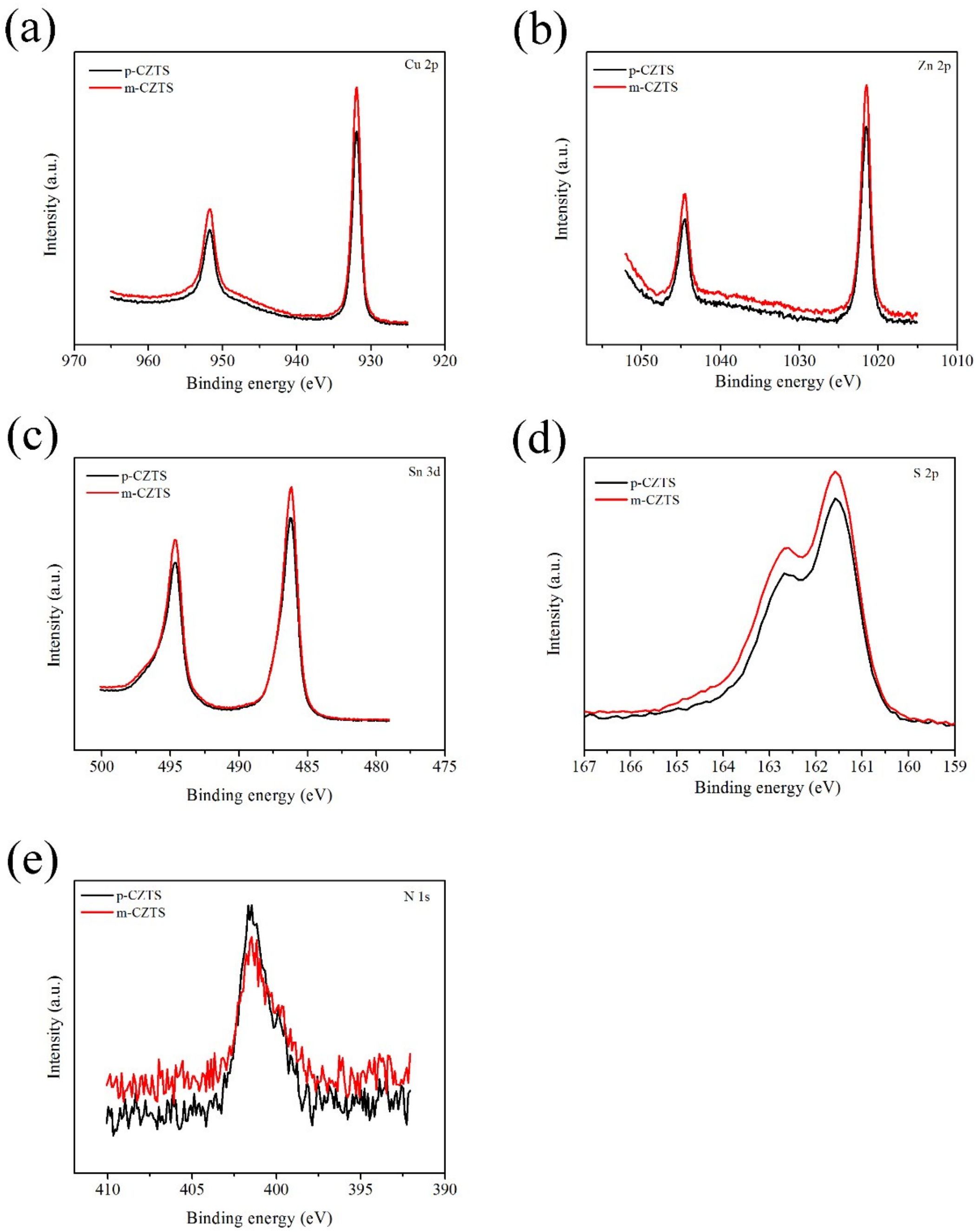

Fig. S1. High resolution core XPS spectra of (a) Cu 2p, (b) Zn 2p, (c) Sn 3d, (d) S 2p, and (d) N 1s for p-CZTS and m-CZTS nanoparticles.

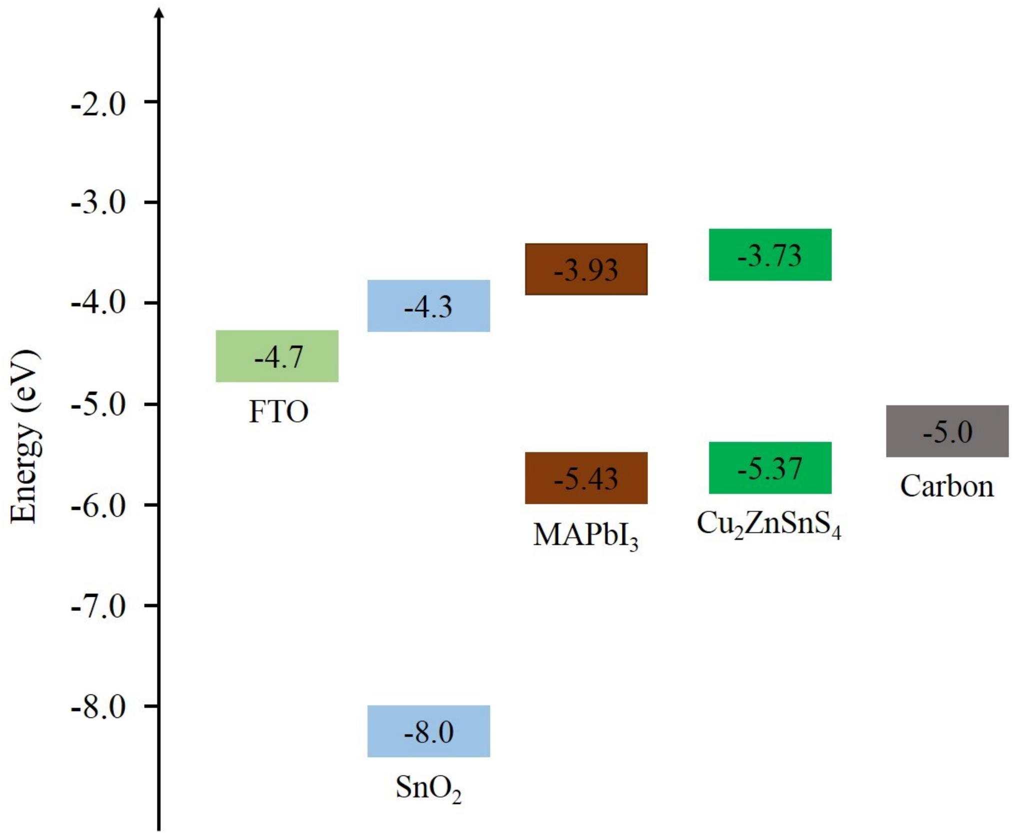

Fig. S2. Energy band diagram of the perovskite solar cells. The band levels of FTO, SnO_2, $MAPbI_3$, Cu_2ZnSnS_4 and Carbon are extracted from references[1, 2].

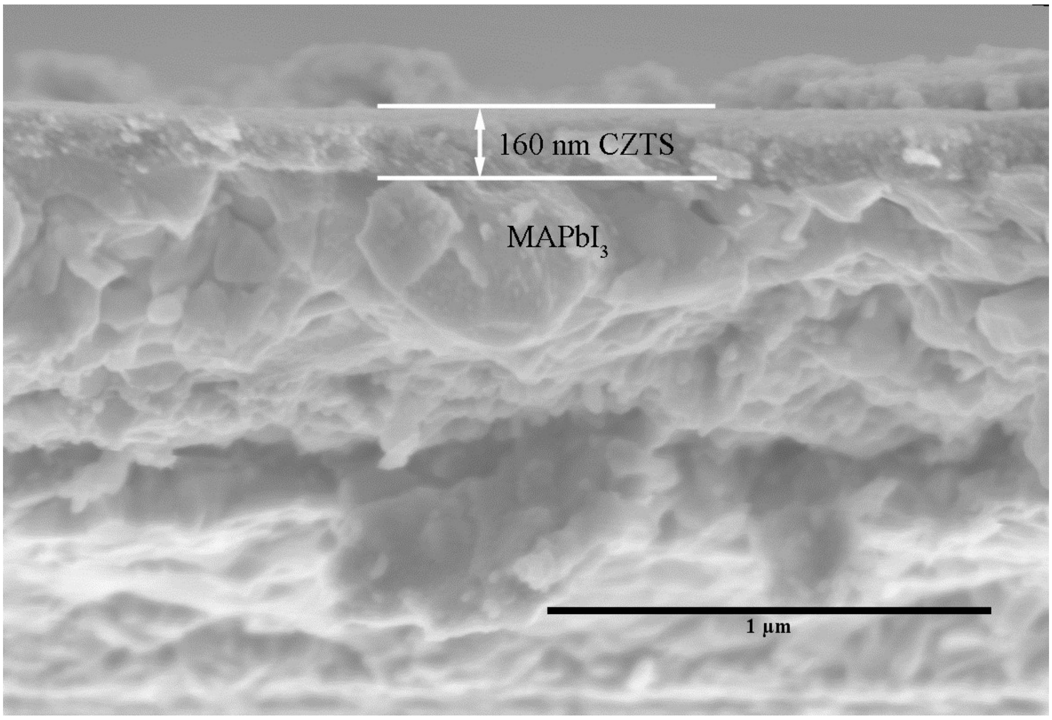

Fig. S3. Cross sectional SEM image of a typical p-CZTS film deposited on $MAPbI_3$. The thickness of p-CZTS film is estimated to be 160 nm.

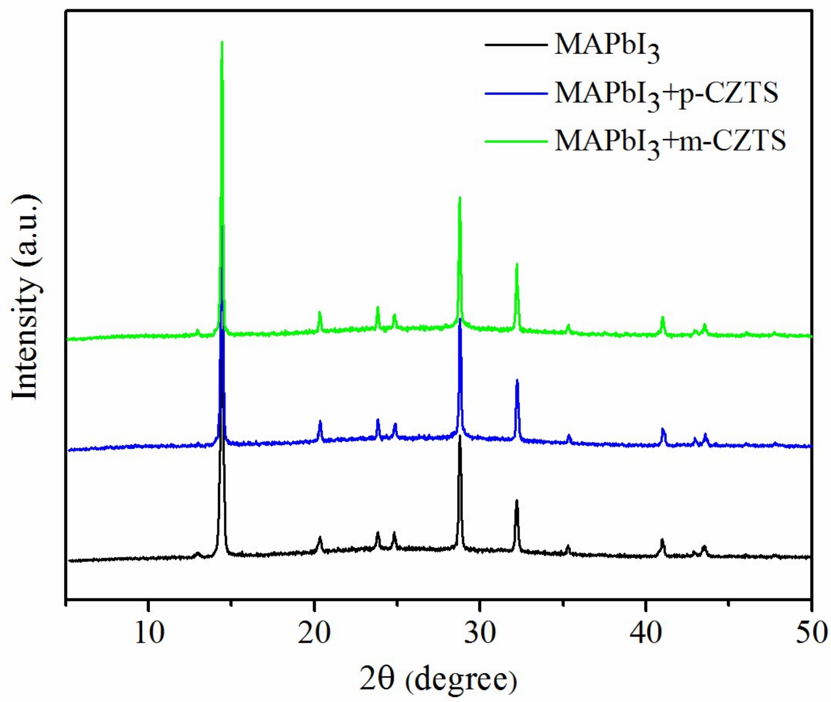

Fig. S4. XRD patterns for $MAPbI_3$ film, $MAPbI_3$/p-CZTS film, and $MAPbI_3$/m-CZTS film.

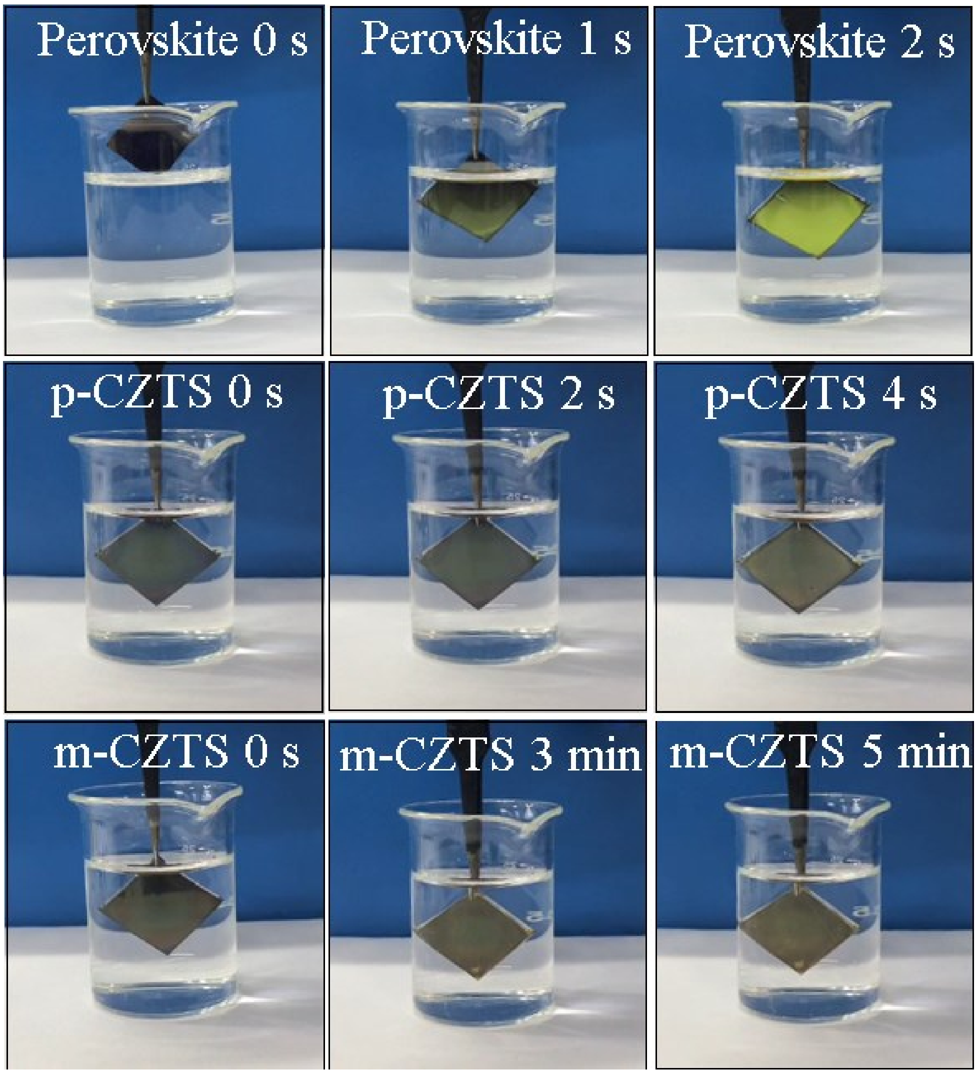

Fig. S5. Stability test of perovskite, perovskite/p-CZTS, and perovskite/m-CZTS films immersed into deionized water. It can be seen from the above figures that bare perovskite film is unstable to water intrusion, and the dark brown perovskite film turns to yellow instantly when immersed into water. When a thin p-CZTS layer is deposited onto the perovskite film, the perovskite/p-CZTS film is more robust and starts to turn yellow after 4 s in the water. When a thin m-CZTS layer is deposited onto the perovskite film, the perovskite/m-CZTS film remains dark brown color for 5 min in the water. This simple test demonstrates that the m-CZTS film can protect the perovskite film from water degradation, and therefore ensures better device stability of the corresponding perovskite solar cell.

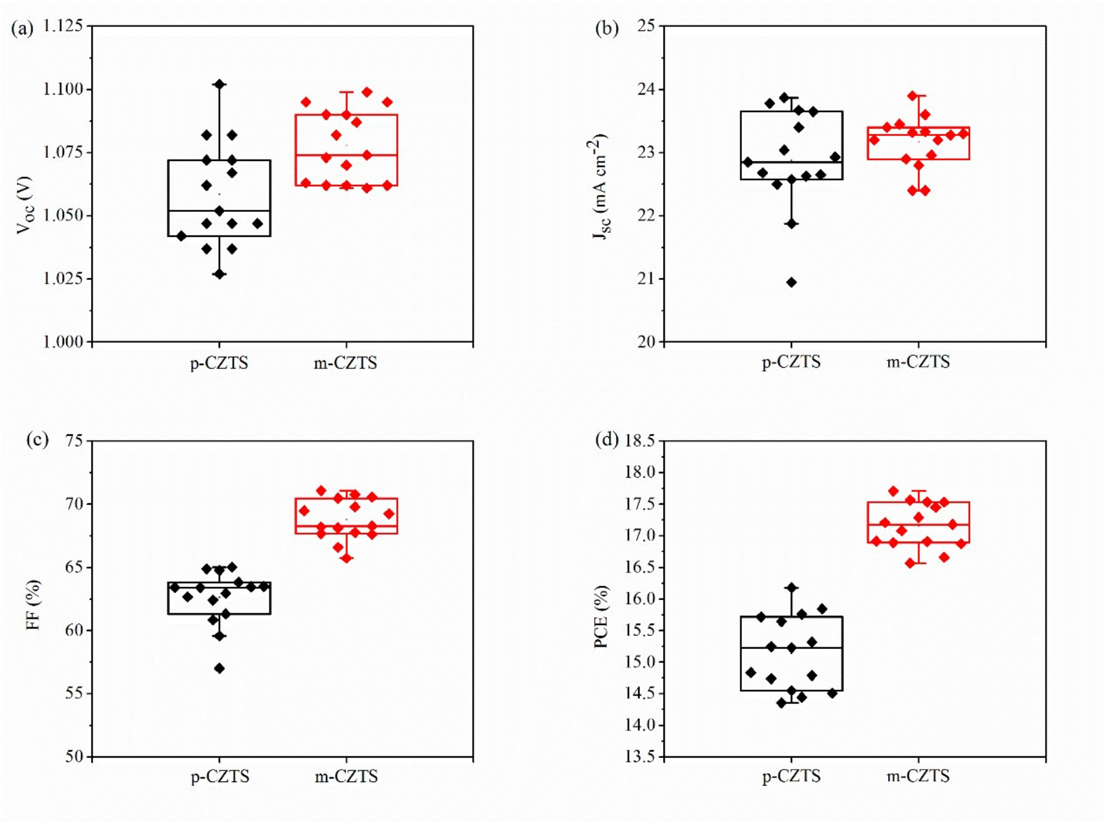

Fig. S6. Statistical photovoltaic parameters (a) V_{oc}, (b) J_{sc}, (c) FF, and (d) PCE for $FAPbI_3$ perovskite solar cells employing both p-CZTS and m-CZTS hole transporting layer.

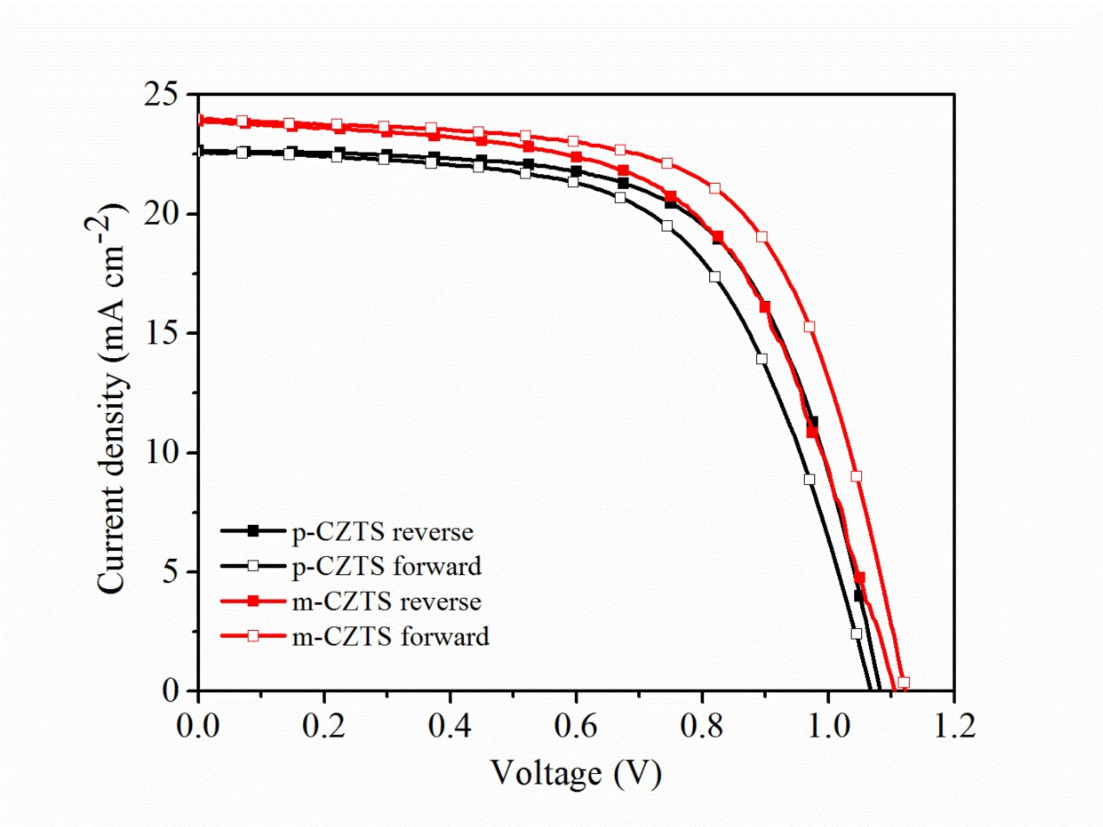

Fig. S7. Typical J-V curves for $FAPbI_3$ perovskite solar cells employing both p-CZTS and m-CZTS hole transporting layers.

Table S1. Atomic percentages calculated from the XPS measurement.

Sample	Element	Area (N)	Atomic percentage (%) without N	Atomic percentage (%) with N
p-CZTS	Cu 2p3	1926.95	21.5	20.0
	Zn 2p3	688.36	7.7	7.2
	Sn 3d	1320.73	14.7	13.7
	S 2p	5025.42	56.1	52.3
	N 1s	650.05	--	6.8
m-CZTS	Cu 2p3	2338.53	22.8	21.8
	Zn 2p3	795.19	7.7	7.4
	Sn 3d	1453.93	14.1	13.6
	S 2p	5697.46	55.4	53.1
	N 1s	438.03	--	4.1

Table S2. Statistical photovoltaic parameters (a) V_{oc}, (b) J_{sc}, (c) FF, and (d) PCE for $FAPbI_3$ perovskite solar cells employing both p-CZTS and m-CZTS hole transporting layer. The average and standard deviation are calculated from 15 samples for each kind of perovskite solar cells.

	V_{oc} (V)	J_{sc} (mA cm^{-2})	FF (%)	PCE (%)
p-CZTS	1.058±0.021	22.87±0.78	62.61±2.16	15.14±0.59
m-CZTS	1.078±0.014	23.16±0.41	68.76±1.59	17.16±0.35

Table S3. Summary of power conversion efficiencies for perovskite solar cells employing a hole transporting layer and carbon electrode. Preparation method for each hole transporting layer and carbon electrode is also given in the parenthesis.

Hole transporting layer	Carbon electrode	Champion PCE	Reference
Spiro-OMeTAD (Spin-coating + Drop-casting)	Single-walled carbon nanotube (Press-transfer)	16.6%	[3]
Spiro-OMeTAD (Spin-coating)	Modified commercial carbon paste (Press-transfer)	19.2%	[4]
Spiro-OMeTAD (Spin-coating)	Graphene (Spraying + Press)	18.65%	[5]
CuPc (thermal evaporation)	Commercial carbon paste (Doctor-blading)	16.1%	[6]
CuPc (thermal evaporation)	Commercial carbon paste (Doctor-blading)	17.46%	[7]
CuPc-TIPS (Spin-coating)	Commercial carbon paste (Doctor-blading)	14.0%	[8]
CuSCN (Spin-coating)	Multi-walled carbon nanotube (Drop-casting)	17.58%	[9]
Cu_2ZnSnS_4 (Spin-coating)	Modified Commercial carbon paste (Doctor-blading)	17.71%	Our work

References:

[1] M. Yuan, X. Zhang, J. Kong, W. Zhou, Z. Zhou, Q. Tian, Y. Meng, S. Wu, D. Kou, Controlling the Band Gap to Improve Open-Circuit Voltage in Metal Chalcogenide based Perovskite Solar Cells, Electrochimica Acta, 215 (2016) 374-379.

[2] P.-K. Kung, M.-H. Li, P.-Y. Lin, Y.-H. Chiang, C.-R. Chan, T.-F. Guo, P. Chen, A Review of Inorganic Hole Transport Materials for Perovskite Solar Cells, Advanced Materials Interfaces, 5 (2018) 1800882.

[3] K. Aitola, K. Domanski, J.-P. Correa-Baena, K. Sveinbjörnsson, M. Saliba, A. Abate, M. Grätzel, E. Kauppinen, E.M.J. Johansson, W. Tress, A. Hagfeldt, G. Boschloo, High Temperature-Stable Perovskite Solar Cell Based on Low-Cost Carbon Nanotube Hole Contact, Advanced Materials, 29 (2017) 1606398.

[4] H. Zhang, J. Xiao, J. Shi, H. Su, Y. Luo, D. Li, H. Wu, Y.-B. Cheng, Q. Meng, Self-Adhesive Macroporous Carbon Electrodes for Efficient and Stable Perovskite Solar Cells, Advanced Functional Materials, 28 (2018) 1802985.

[5] C. Zhang, S. Wang, H. Zhang, Y. Feng, W. Tian, Y. Yan, J. Bian, Y. Wang, S. Jin, S.M. Zakeeruddin, M. Grätzel, Y. Shi, Efficient stable graphene-based perovskite solar cells with high flexibility in device assembling via modular architecture design, Energy & Environmental Science, (2019).

[6] F. Zhang, X. Yang, M. Cheng, W. Wang, L. Sun, Boosting the efficiency and the stability of low cost perovskite solar cells by using CuPc nanorods as hole transport material and carbon as counter electrode, Nano Energy, 20 (2016) 108-116.

[7] X. Liu, Z. Liu, B. Sun, X. Tan, H. Ye, Y. Tu, T. Shi, Z. Tang, G. Liao, 17.46% efficient and highly stable carbon-based planar perovskite solar cells employing Ni-doped rutile TiO_2 as electron transport layer, Nano Energy, 50 (2018) 201-211.

[8] X. Jiang, Z. Yu, H.-B. Li, Y. Zhao, J. Qu, J. Lai, W. Ma, D. Wang, X. Yang, L. Sun, A solution-processable copper(ii) phthalocyanine derivative as a dopant-free hole-transporting material for efficient and stable carbon counter electrode-based perovskite solar cells, Journal of Materials Chemistry A, 5 (2017) 17862-17866.

[9] X. Wu, L. Xie, K. Lin, J. Lu, K. Wang, W. Feng, B. Fan, P. Yin, Z. Wei, Efficient and stable carbon-based perovskite solar cells enabled by the inorganic interface of CuSCN and carbon nanotubes, Journal of Materials Chemistry A, 7 (2019) 12236-12243.